

## PAPER

View Article Online  
View Journal | View Issue



Cite this: *Ind. Chem. Mater.*, 2023, 1, 431

# A highly efficient photocatalytic system for environmental applications based on TiO<sub>2</sub> nanomaterials

Sapanbir S. Thind,<sup>ab</sup> Mathias Paul,<sup>a</sup> John B. Hayden,<sup>b</sup> Anuj Joshi,<sup>iD c</sup> David Goodlett<sup>c</sup> and J. Scott McIndoe<sup>iD \*a</sup>

Sustainable and efficient water treatment techniques to improve the quality of water for various applications include advanced oxidation processes (AOP), mainly focusing on heterogeneous photocatalysis. Materials science and nanotechnology have contributed to tailoring the properties of photocatalytic materials to significantly enhance their photoactivity and stability. Here we report the development of a well-organized nanoporous TiO<sub>2</sub>-based photocatalytic reactor for water treatment. Nanoporous TiO<sub>2</sub> materials were directly grown using a two-step electrochemical anodization process in ethylene glycol + 0.3 wt% NH<sub>4</sub>F + 2 wt% H<sub>2</sub>O. The prepared nanomaterials were characterized by X-ray diffraction (XRD), scanning electron microscope (SEM), and energy-dispersive X-ray spectroscopy (EDX). To enhance the photocatalytic activity of the system, water scrubbing was incorporated to boost the presence of oxygen in the water, enhancing the electron uptake at the conduction band thus significantly reducing the electron-hole recombination and increasing the photocatalytic activity. To further enhance the efficiency and reduce the negative environmental impact of the technology, a UVA-LED assembly was used instead of the typical mercury-based UV lamps for photocatalysis. The nanoporous TiO<sub>2</sub> was tested as a catalyst for the photochemical oxidation of various categories of pollutants; dye (methylene blue), and the removal of microbes such as *E. coli*. The photoreactor developed in this research work was also successfully applied and tested in real-world applications such as keeping heavily used hot-tub water clean without using harmful chemicals (chlorine, bromine, ozone, etc.) or expensive equipment. The simplicity and efficacy of the new approach described in this study make possible the integration of nanoporous TiO<sub>2</sub> in the design of high-performance air and water purification technologies.

**Keywords:** TiO<sub>2</sub> photocatalyst; UVA-LEDs; Nanostructured materials; Photochemical oxidation; Wastewater treatment; Water scrubbing.

Received 11th May 2023,  
Accepted 7th June 2023

DOI: 10.1039/d3im00053b

rsc.li/icm

## 1 Introduction

The progressive degradation of water quality has become a critical issue globally, due to the rapid pace of industrial development and the cumulative discharge of myriad contaminants into ecosystems *via* wastewater.<sup>1</sup> Wastewater from industries can contain toxic chemicals, heavy metals, microorganisms, biological substances, microplastics, and oils.<sup>2,3</sup> In its 2017 report, the United Nations Educational, Scientific and Cultural Organization (UNESCO) reported that more than 80% of the industrial wastewater that is not

treated at all is released into various bodies of water.<sup>4</sup> The textile industry is one of the biggest polluters of fresh water and it is believed that approximately 20 percent of all freshwater pollution is caused during textile treatment and dyeing. The global textile and clothing industry remains the major contributor to water pollution in the 21st century.<sup>5,6</sup> The treatment of wastewater has been extensively studied by several conventional remediation techniques such as physical methods, flocculation, reverse osmosis, biological methods, thermal and chemical methods, and high-energy UV light. All these methods are not only limited to treating most of the compounds,<sup>7</sup> they also have a high operating cost over the long-term, consume a large amount of energy, only partially decompose the pollutants (leaving byproducts of unknown toxicity), and transfer the organic pollutant from one phase to another phase resulting in the formation of a secondary pollutant, which necessitates further treatment.<sup>8</sup> In recent

<sup>a</sup> Department of Chemistry, University of Victoria, 3800 Finnerty Road, Victoria, BC, V8P 5C2 Canada. E-mail: mcindoe@uvic.ca

<sup>b</sup> Waterdrape LLC, Paradise Valley, Arizona, USA

<sup>c</sup> Genome BC Proteomics Centre, University of Victoria, Victoria, British Columbia, Canada



years, great effort has been made to develop clean and inexpensive heterogeneous photocatalysts for the elimination of myriad pollutants from wastewater.<sup>9–12</sup> Photocatalysis has also gained importance due to its versatility in having a broad spectrum of applications.<sup>13,14</sup> For a heterogeneous catalytic process, there is no need for a continuous supply of precursor chemicals, which is a striking benefit in some applications particularly those in remote or resource-limited locations.<sup>15</sup> There are thousands of research articles published in the last couple of decades on heterogeneous photocatalysis,<sup>10,15–18</sup> which shows that the scientific community has huge optimism about this technology. Among various oxide semiconductor photocatalysts, titanium dioxide (TiO<sub>2</sub>) is considered one of the best materials for the degradation of hazardous pollutants due to its strong oxidizing power, high photocatalytic activity, chemical, and biological stability, relatively low cost, nontoxicity, and long-term photostability.<sup>19–26</sup> Photocatalysis on TiO<sub>2</sub> in water has been conventionally considered a non-selective process but there are new studies that are investigating selective photocatalysis.<sup>27</sup> TiO<sub>2</sub> with different morphologies such as nanospheres, nanotubes, nanorods, nanofibers, and nanowires have been reported for the removal of pollutants from water.<sup>28–31</sup>

Even with all the above-mentioned capabilities, photocatalytic-based AOP systems are scarce in the commercial market for water treatment applications. One of the main reasons there is a huge gap between the literature and commercial products is the scalability issue. All the research work is done at a bench scale, with very small dimension photocatalytic systems employed and typically only a few milliliters of water treated. During the application period, the technology faces various limitations due to up-scaling issues. Researchers have also put much emphasis on developing new materials with more complex morphologies and performing doping and co-doping. Doping with transition metals (*e.g.* Fe, W, Cr, and V) and non-metal dopants (*e.g.* N, C, F, and S) helps in decreasing the bandgap and creating oxygen vacancies or low-lying interband states at the localized energy levels of the dopant.<sup>32–35</sup> This slight increase in the activity of the photocatalyst under visible light has not been enough to solve the commercialization challenges. It is also proven that doping of TiO<sub>2</sub> does not provide a long-term enhancement in the activity and suffers from instability issues. Chadwick *et al.* have reported that interstitially nitrogen (N<sub>i</sub>) doped TiO<sub>2</sub> suffers from environmental UVA irradiation-induced dopant surface segregation and the dopants are then irreversibly lost through subsequent photo-induced reaction pathways.<sup>36</sup> Doping, and co-doping also make the fabrication of nanomaterials more tedious and expensive.

Various factors which limit the design of photocatalytic reactors for environmental remediation include size, effective cost, process time, and light source.<sup>37,38</sup> Photocatalytic reactors solely dependent on utilizing classical ultraviolet (UV) excitation sources have limited applications due to many

inherited problems such as i) the harmful side effect of UV sources, ii) its power instability during long time operation, iii) low photonic efficiency, operating conditions such as the high voltage at the initial stage, cooling requirement, high vapor pressure, and usage of hazardous mercury metal.<sup>38</sup> Another problem associated with classical UV lamps is their shorter lifetime and broader spectral wavelength.<sup>39</sup> Mercury metal is one of the hazardous air pollutants (HAP) specified by the U.S. Environmental Protection Agency. Exposure to mercury vapors can also lead to several health complications such as damage to the eye, kidneys, brain, and skin.<sup>40</sup> This is one of the main reasons why much effort has been devoted to finding an alternative safer source for exciting the photocatalyst. It is a priority to move towards a renewable source of energy, and thus solar light-based photocatalytic reactors are garnering much attention. Although solar light-based technology is hygienic, renewable, and sustainable, there are challenges associated with it such as its high cost and the large area for installation. Solar light is not available all the time and its intensity varies throughout the day resulting in inefficient photocatalysis. The solution to these problems is the development of UVA light-emitting diodes (LED) in which the flow of current in LED is one-directional (forward-biased), and it emits UV light in a narrow spectrum in the form of electroluminescence. There is no wastage of light energy in these UVA LEDs as only the required wavelength is emitted. The lifespan of these LEDs is another advantage as they last at least 100 times as long as a typical gas-discharge UV bulb. UV-LED sources have high robustness, less heat generation, good linearity of the emitted light intensity with current, suitability for operation in a pulsed regime at high frequencies, are easily portable, and have a small size compatible with the modern trend in the design of the miniaturized photocatalytic reactor.<sup>38</sup>

Another challenge with TiO<sub>2</sub>-based photoreactors is that most of the research work is focused on powder-based materials. On a lab scale, it is easy to centrifuge the powder nanomaterials after the photocatalytic oxidation of the pollutant but on a large scale where thousands of liters of water need to be treated, it becomes difficult to pour that much powder-based photocatalyst in the water and then make sure all of it is filtered out before discarding the treated water back in the environment. Such a process is very expensive and complicated. If any of these nanomaterials pass through the filter system, it can cause secondary pollution and harm to the environment.<sup>41</sup> These slurry-based photocatalytic reactors also are very inefficient as when the system is irradiated with UV, it is almost impossible to irradiate each particle as the light gets scattered from the particles present close to the light source. The particles far away and/or blocked do not get enough photons to get the electron excitation going and thus the overall efficiency of the system is much reduced. Some researchers have suggested applying these powdered nanomaterials on a surface either by painting or by sputtering methods however no long-term adhesion can be achieved and with time they



lose connectivity, and the material starts falling from the supporting material.

We have used electrochemical anodization to directly grow  $\text{TiO}_2$  nanoporous material on the titanium metal substrate. As these nanoporous materials are made by etching holes in the titanium metal by the fluoride ions present in the electrolytic solution, they are an integral part of the metal substrate, are very stable, and are not prone to detachment. There are research works where electrochemically grown  $\text{TiO}_2$  nanoporous/nanotube materials are used for various applications such as solar cells, photocatalysis, gas sensors, functional surface devices, supercapacitors, and water splitting.<sup>42–44</sup> This anodized nanoporous material also possesses the scattering nature of free electrons, high surface area, better light absorption efficiency, and enhances electron mobility, which offers superior charge transport leading to higher photocatalytic efficiency.<sup>45–48</sup>

Another major roadblock in the development of photocatalysis-based water treatment technologies is the low photoconversion efficiency resulting from electron-hole recombination.<sup>49</sup> When the electron gets excited from the valence band to the conduction band after the absorption of the photons, it needs to react with the oxygen molecule present in the water. Unfortunately, a very high number of the excited electrons fall back to the valence band and recombine with the holes, resulting in less photocatalytic activity as these holes are no longer available to react with water molecules and generate hydroxyl radicals. In our patented technology, we have incorporated water scrubbing into the system which ensures that there is no oxygen shortage in the solution. It is well noted that the presence of electron-capturing species enhances photocatalytic activity by reducing electron-hole recombination.<sup>50</sup>

In the present work, we have developed a novel patented photoreactor that employed highly organized  $\text{TiO}_2$  nanoporous material as a photocatalyst and a highly energy-efficient UVA-LED assembly for irradiation. Water scrubbing was also used to keep the photoreactor saturated with oxygen thus reducing electron-hole recombination. The photoreactor was tested for real-world applications such as cleaning hot tubs without employing any chemicals. Our experimental results show that the manufactured photoreactor was highly active and very efficient in the water treatment. It is a next-generation photocatalytic system that is lightweight and easily portable.

## 2 Results and discussion

### 2.1 Morphology of synthesized materials

$\text{TiO}_2$  nanotubes/nanoporous structures are extremely attractive for photocatalytic applications because of their large surface area, high physical stability, good adsorption ability, superior electron transport rate, and excellent photoelectrochemical properties.<sup>51</sup> Nanotubular  $\text{TiO}_2$  geometries are also especially attractive for photocatalytic

applications due to their directionality to light and charge management. It is proven that regular spacing between  $\text{TiO}_2$  nanotubular structures leads to better light-trapping characteristics and faster charge transfer behavior.<sup>52</sup> It is also convenient to employ these types of structures for photocatalysis compared to powder materials.<sup>53,54</sup> Fig. 1 shows how spherical nanopowders are very limited in utilizing the irradiation as compared to the tubular structure where light trapping results in more surface area of the  $\text{TiO}_2$  being irradiated and thus resulting in higher photocatalytic efficiency. Therefore, the synthesis of  $\text{TiO}_2$  nanotubular structure for photocatalytic applications has gained the interest of the research community attempting to find a solution for water treatment. These types of tubular structures can be prepared by various methods such as hydrothermal, sol-gel, template-assisted, and electrochemical anodization methods.<sup>55–60</sup> The electrochemical anodization method for the fabrication of  $\text{TiO}_2$  nanotubes has several advantages over other methods. The anodization method is quick, and the morphology of the nanotubes can be controlled by regulating experimental conditions such as oxidation electrode potential, the concentration of the electrolyte, and anodization time.<sup>61,62</sup> Different lengths and thicknesses of the nanotubular materials can be achieved by the anodization method.

In this work, highly ordered nanoporous  $\text{TiO}_2$  was directly grown on a titanium surface using electrochemical oxidation in ethylene glycol with  $\text{NH}_4\text{F}$  and  $\text{H}_2\text{O}$ . The structure and morphology of the formed  $\text{TiO}_2$  were characterized *via* SEM. As shown in Fig. 2a, highly ordered nanopores were uniformly generated on the Ti substrate. A higher resolution SEM image is presented in Fig. 2b, which revealed that the diameter of the nanopores was *ca.* 150 nm and that each nanopore consisted of several smaller nanopores.

It was obvious that the lumina of the pores were exposed at the top of the layer. Our final anodization time was adjusted to 15 minutes after optimization, which could provide more uniform growth without notable deformities, and the nanomaterials were less prone to detachment and

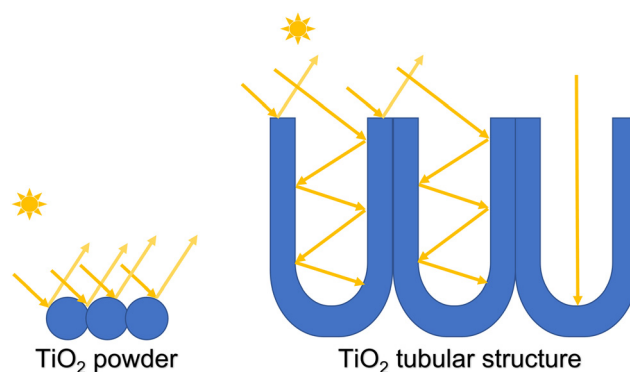


Fig. 1 Comparison between the spherical nanopowder  $\text{TiO}_2$  vs. tubular  $\text{TiO}_2$  toward light distribution.



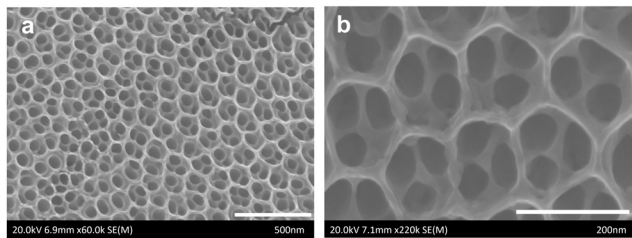


Fig. 2 (a) Low, and (b) high magnification SEM images of prepared TiO<sub>2</sub> nanoporous materials.

more tenaciously adhered to the substrate. It is well known that the surface area of catalysts plays a significant role in their catalytic activity.<sup>63</sup> A higher surface area might provide many more additional active sites for catalysis. The nanomaterials fabricated in this study possessed a very high surface area, as was evidenced by the wide openings at the top of the layer, which provided additional sites for catalytic reactions to occur. To determine the crystalline structure of the nanoporous TiO<sub>2</sub>, XRD spectra were collected and compared with PANalytical ICSD database. TiO<sub>2</sub> exists primarily in three main phases: anatase, brookite, and rutile. Among these phases, rutile is the most stable phase as a bulk material, and synthesis methods that involve annealing up to 500 °C mostly result in the anatase structure. The synthesis of TiO<sub>2</sub> at nanometric dimensions also favours the anatase

phase over rutile and brookite, as the surface energy of anatase is lower than the other phases. The anatase phase is also the most catalytically active phase among TiO<sub>2</sub> phases. As shown in Fig. 3a, two diffraction peaks centered at  $2\theta$  angles of 25.4 and 48.0 were observed for the prepared TiO<sub>2</sub> nanoporous material confirming that TiO<sub>2</sub> is present in the desired anatase phase. The peaks marked with asterisks are derived from the Ti substrate. Strong oxygen and titanium peaks at a ratio of 2:1 were observed in the EDX (Fig. 3b), which again confirmed the formation of the TiO<sub>2</sub> nanoporous arrays.

## 2.2 Photocatalytic oxidation of methylene blue (target pharmaceutical waste)

Pharmaceutical industries release wastewater containing drugs especially antibiotics into water bodies causing serious water pollution.<sup>64,65</sup> Even the wastewater from households contains a significant number of drugs entering the environment. Due to advances in medical science, now there is a drug for most diseases and large quantities of different pharmaceutical drugs are produced each year. Unfortunately, many expire unused, and these pharmaceuticals can find their way into the environment due to improper disposal. Wastewaters containing pharmaceutical drugs pose a serious threat to aquatic life. Some municipalities have noticed a measurable number of painkillers in their wastewater. Another negative attribute of pharmaceutical waste is that it is impossible to separate different kinds of pharmaceutical compounds *i.e.*, antibiotics, hormones, steroids, *etc.* through wastewater treatment and cannot be degraded by means of biological treatment. In the last couple of decades, AOP has shown its capability to oxidize pharmaceutical waste into nontoxic organic material. There are many reports in the literature where researchers have used heterogeneous photocatalysis in the successful abatement of pharmaceutical pollutants.

Methylene blue, also known as methylthioninium chloride, is a salt used as a medication and dye. As a medication, it is mainly used to treat methemoglobinemia.<sup>66</sup> In our typical experiment, 20 mg of MB was dissolved in 6 L water and this solution was subjected to photocatalytic oxidation. Samples were taken at regular intervals and the absorbance was measured with the help of UV-vis absorbance spectroscopy. Methylene blue (MB) is a cationic dye that exhibits two major absorption bands at 293 ( $\pi-\pi^*$ ) and 664 ( $n-\pi^*$ ) nm in dilute aqueous solutions, the latter having a shoulder at 610 nm corresponding to the 0-1 vibronic transition. In our studies, we calculated the degradation of MB by studying the decrease in the 664 nm peak. 95% of the MB was photocatalytically oxidized in 4 hours and in 6 hours the UV-vis spectrophotometer read zero absorbance at 664 nm establishing that complete mineralization of the MB is achieved (Fig. 4a). Fig. 4b and c show the colour of water before and after oxidation.

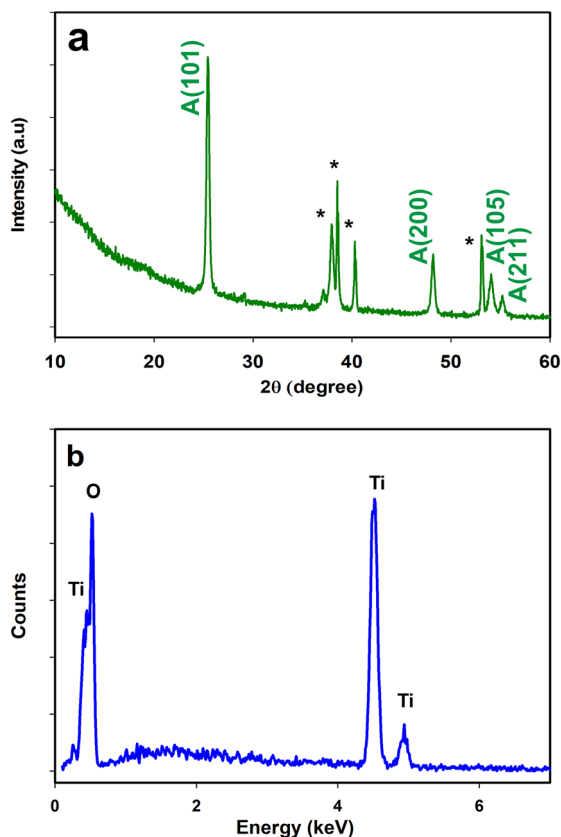


Fig. 3 XRD (a) and EDX (b) of TiO<sub>2</sub> nanoporous material.





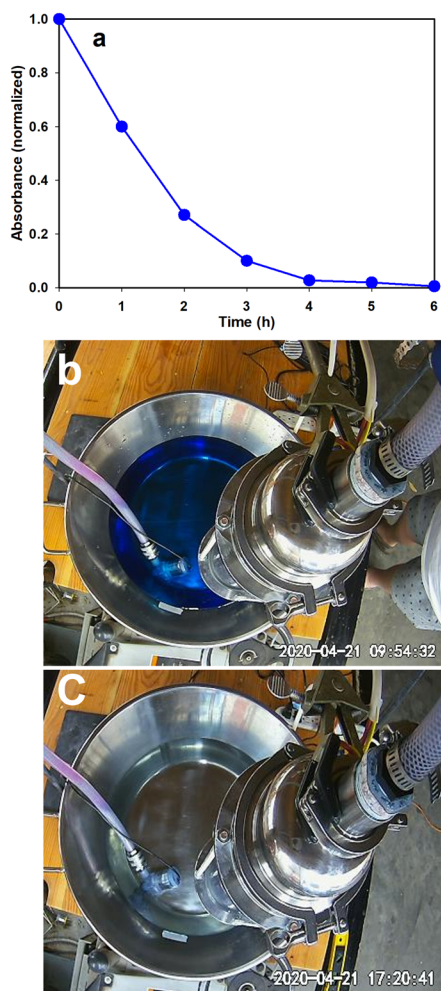


Fig. 4 (a) UV-vis absorbance results during photocatalytic oxidation of MB; pictures showing the colour of MB solution (b) before and (c) after oxidation.

## 2.3 Real-world applications

**2.3.1 Chemical-free hot tub.** To oxidize contaminants in hot tubs, chlorine compounds are the most popular pool sanitizer due to their efficacy and low cost. They are effective at killing viruses, and bacteria, and will also help prevent algae from growing in the first place. When chlorine is added to pool water in the form of sodium hypochlorite, it breaks down into hypochlorite ion and hypochlorous acid, both of which are effective at killing bacteria and various microorganisms. Free chlorine is the amount of chlorine able to sanitize contaminants, while combined chlorine refers to chlorine that has already been combined directly with the contaminants. Total chlorine is the sum of free chlorine and combined chlorine. The user needs to keep adding chlorine in the hot tub because the free chlorine keeps reacting with the microorganisms, oils, dead skin, soap, and everything else humans put on their bodies. The main culprit for the bad smell in the hot tub and pools is chloramines, which build up in a hot tub when it is improperly treated. Chloramines are generated when

chlorine combines with ammonia or other nitrogen sources (perspiration, oils, and urine) that come into the hot tub with the bathers.

About 7.3 million hot tubs are currently operating in the United States right now. There are about 10.4 million residential swimming pools currently used in the United States. Canada represents about a tenth of this number, based on population. A drag on the growth of the hot tub industry is the extensive use of chemicals to sanitize the water. The persistent issue among hot-tub enthusiasts is the chemical odour and the negative health-related issues these chemicals cause. Chlorine and bromine compounds are very effective in keeping the hot tub clean. However, the government of Canada recently deemed the risk to human health from the misuse of sodium bromide by consumers as too dangerous to continue to have it available to individual Canadians. There is a clear need for a chemical-free and environmentally friendly technology that produces no secondary pollution and causes no harm to the health of end users.

A two-month-long experiment was conducted on a heavily used hot tub with a water volume of 1200 L. Before the testing period, the hot tub was completely drained and cleaned to get rid of all the chemicals present. During these two months of testing, no other means of sanitization were used such as salt, ozone, liquid chlorine, bromine, or electrolytic systems that convert added salt into free chlorine. In these two months, 60 bodies (around 10 different users) went in the hot tub and the average usage time per user was between 30 to 40 min. For this experiment, titanium dioxide nanomaterials were grown on the inner surface of a titanium tube with a diameter of *ca.* 11.5 cm and height of 15.25 cm *via* anodization method explained in the experimental section. The geometrical surface area of the photocatalyst is approximately 550 cm<sup>2</sup>. The size of the photocatalytic tube in the photoreactor can be adjusted based on the volume of the water in the hot tub or spa.

Fig. 5 shows the plotted data collected during the test run. Fig. 5a is TOC (Total Organic Carbon) which is a measure of the total amount of carbon in organic compounds in pure water and aqueous systems. The initial tap water TOC was 2.7 ppm and even after two months of heavy use and big bather loads, the TOC remained stable at close to 3.2 ppm. This result shows that the photocatalytic reactor was able to completely oxidize most of the organic compounds entering the water. When not maintained and cleaned properly, hot tubs provide an ideal environment for bacteria and viruses to grow, causing skin, eye, and ear infections, as well as other serious diseases. In our study, COD (Chemical Oxygen Demand) was also regularly measured and can be used as a general indicator of water quality (Fig. 5b). Biochemical Oxygen Demand (BOD) can be estimated from COD measurements and represents the amount of oxygen consumed by bacteria and other microorganisms while they decompose organic matter under aerobic (oxygen is present) conditions at a specified temperature. In general, a higher



COD or BOD value means the water has bacterial growth in it. In our testing, no significant increase in the COD value was observed even with a very high bather load showing that the photocatalytic reactor was able to keep the bacterial growth under control. The photoreactor oxidizes organic materials eliminating the nutrient media for the bacteria. It also directly oxidizes already present or introduced pathogens through photocatalytic oxidation. It was however noticed that a constant increase in the Total Dissolved Solids (TDS) was observed which represents the total concentration of dissolved substances in water (Fig. 5c). Common inorganic salts that can be found in water include calcium, magnesium, potassium, and sodium cations, and carbonate, bicarbonate, nitrate, chloride, and sulfate anions. The initial water has TDS value of  $20 \text{ mg L}^{-1}$  and the hot tub water after two months of usage and photocatalytic treatment has a value of around  $120 \text{ mg L}^{-1}$ . This increase is most likely due to the addition of different cations and anions present in the

human sweat (primarily NaCl). The value is still safe as according to EPA USA up to  $500 \text{ mg L}^{-1}$  is good for drinking.

Bacterial studies were performed on treated hot tub water to ensure user safety. Hot tub water (20 ml) was collected in falcon tubes and centrifuged for 15 minutes. The supernatant was discarded, and the pellet was suspended in  $500 \mu\text{L}$  of LB.  $10 \mu\text{L}$  of the resuspension was plated on LB agar and incubated. Bacteria were identified using FLAT. One  $\mu\text{L}$  of citric acid buffer was added to each well on a matrix-assisted laser desorption ionization mass spectrometry (MALDI-MS) plate. Colonies were picked from the LB agar plate and resuspended in a buffer. The plate was incubated at  $110^\circ\text{C}$  for 30 minutes, then washed with sterile deionized water. FLAT analysis (Fig. 6) revealed very little bacterial growth in hot tub water, even after two months of heavy use. The slight growth on the plate shown in Fig. 6b could not result in any FLAT analysis database match. This indicates that it is a reminiscent by-product of the oxidation products of *P. aeruginosa* bacteria. The above results revealed that even after two months of constant heavy usage, the hot tub water was very clean, and almost no bacterial growth was observed.

It can be concluded that the photocatalytic reactor is very efficient in oxidizing different types of pollutants present in the water. Upon UVA irradiation, the excited electrons are captured by the adsorbed  $\text{O}_2$  to give  $\text{O}_2^{\cdot-}$ , and the water molecules adsorbed on the surface of the catalyst react with the hole(+) vacancies to give  $\text{OH}^\cdot$ .<sup>24</sup> The presence of dissolved oxygen plays an important part in generating reactive oxygen species during photocatalysis. Finally, these active oxygen species attack the pollutants and decompose them. The proposed sequential mechanism is as follows.

(a) Absorption of energy

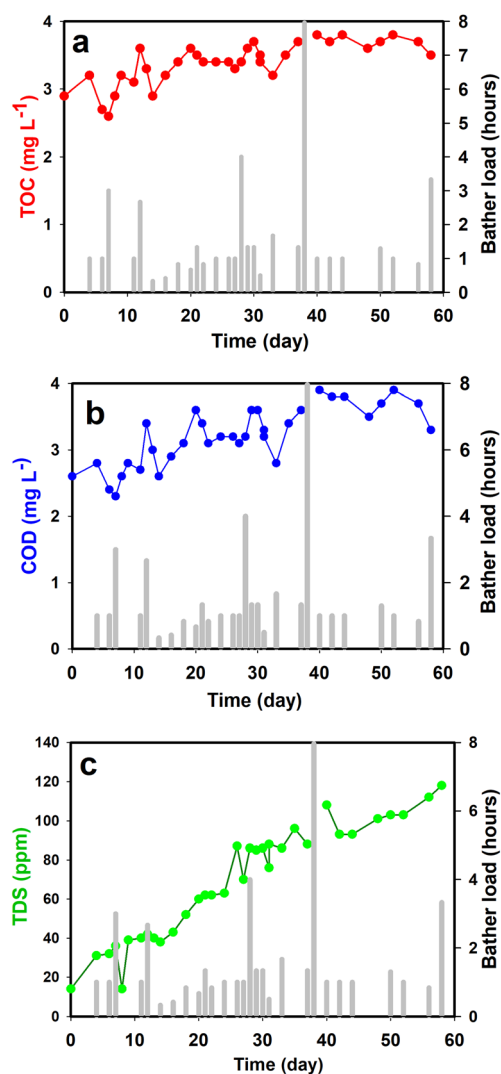


Fig. 5 (a) TOC; (b) COD; and (c) TDS data during the two-month experiment in the hot-tub. The bar graph in each plot is the bather load in hours.

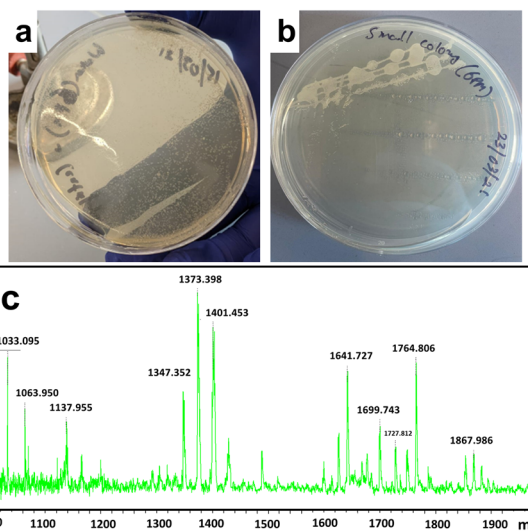


Fig. 6 (a) and (b), assessment of the photocatalytic activity towards disinfection efficiency through the spread plate method; (c) results from FLAT analysis.



## (b) Generation of active oxygen species



## (c) Oxidation of pollutants



As the hydroxyl radicals and other ROS produced by the photocatalytic system are released in the water from the surface of the photocatalyst, only the material dissolved in the water gets oxidized such as oils, lotions, and other organic materials. The solids such as dander, hairs, and soil particles are taken care of by the mechanical filtration system present in the hot tub. Mechanical filtration also helps in protecting the pump and the heating mechanism from unwanted foreign material.

As a control experiment, another long-term experiment was performed where the photocatalytic reactor system was taken out and no sanitization method was used to see how long the water in the hot tub could stay usable. In a couple of weeks, the TOC and COD values started going above 4 ppm, and after a month of usage, the water sample from the hot tub showed very vibrant bacterial growth (Fig. 7). Both these bacteria, *Klebsiella* and *Yersinia*, can cause illness in humans.<sup>67,68</sup> These results show how important the role of sanitization in hot tubs is.

Two of the main reasons for the lack of hot-tub industry growth are maintenance and chemical use. The presented technology is aimed squarely at the heart of this issue. By combining emerging technologies, we can deliver affordable, durable, and easily deployable water purification solutions. The technology is an eco-friendly alternative where the photocatalytic process produces hydroxyl radicals which are much more reactive than chlorine and thus more effective. Another benefit of utilizing heterogenous-based photocatalysis for water treatment is that these hydroxyl radicals are so short-lived they do not cause any harm to the human body. This hydroxyl radical generates different ROS which act as persistent sanitizers for the hot tub surfaces, filtration media, and the bulk of the water. Unlike chlorine, the hydroxyl radical does not generate any secondary pollution and therefore is environmentally friendly. Using photocatalyst-based water treatment systems in the hot tub and pool maintenance context will result in a significant reduction in exposure to chemicals and no release of high concentrations of chemicals into bodies of water and the environment. No need for UVC mercury lamps which cause significant pollution when discarded.

**2.3.2 Bacterial disinfection study.** Most currently adopted water treatment approaches suffer from high chemical/energy demands and require post-treatment to remove undesired chemical by-products. Chlorination comprises one of the most cost-effective methods of disinfection; however, it can generate carcinogenic disinfection by-products (DBPs) during the disinfection process.<sup>69–71</sup> Concerning the safety issues related to chlorination, alternative safe green methods have attracted great interest in water disinfection. Photocatalysis has garnered considerable attention owing to its promising applications in water disinfection and hazardous waste remediation.

An independent bacterial disinfection study was performed using *Escherichia coli* DH5 $\alpha$ . 1.5 L of *E. coli* DH5 $\alpha$  bacterial suspension was prepared from single colony inoculation. A single colony of *E. coli* was spiked into 5 mL LB broth (BD Difco) and incubated at 37 °C for 16 h with continuous shaking at 180 rpm. The *E. coli* culture was added to 145 mL of LB broth and incubated for a further 16 h under the same conditions. Absorbance after the second incubation was 0.282. The culture was centrifuged, the supernatant was discarded, and the pellet was resuspended in 2 L of sterile deionized water.

As a control, a 40 mL aliquot of the suspension was collected prior to filling the photocatalytic reactor. The reactor was filled with suspension and turned on. The sample line was flushed, and a 5 mL sample was collected at 0 hours, 2 hours, and 4 hours. A 1 mL aliquot of each prototype sample and the control were serially diluted to 10<sup>−6</sup> at each time point. 100  $\mu\text{L}$  of undiluted, 10<sup>−4</sup>, and 10<sup>−6</sup> were spread-plated in triplicate on LB agar (BD Difco, Fisher Bioreagents) and incubated for 24 h at 37 °C. Following incubation, CFU mL<sup>−1</sup> was determined. After two hours of water treatment, no colonies were visible. CFU mL<sup>−1</sup> of the control remained

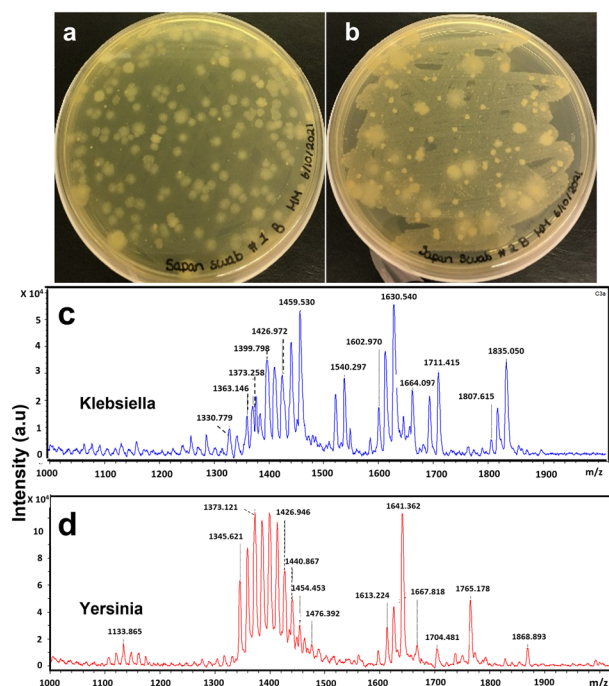
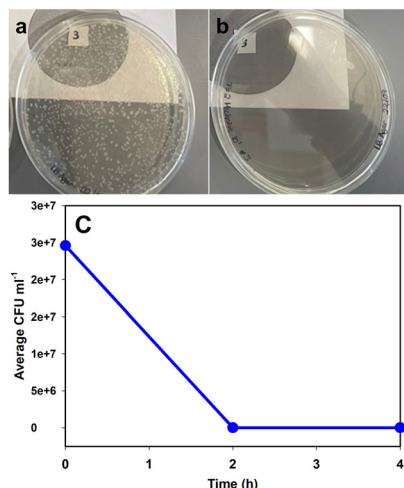


Fig. 7 Bacterial growth study in the hot tub water without any sanitization. (a) and (b) are the results from the spread plate method. (c) and (d), results from FLAT analysis.







**Fig. 8** Results of the spread plate technique for the initial sample (a) and after two hours of photocatalytic oxidation (b); (c) plot confirming the reduction in the bacterial count.

constant over 4 hours. This shows the efficacy of the developed technology in the disinfection of water. This technology can be easily employed in remote areas where there is a shortage of clean drinking water. Fig. 8a shows the numerous CFU present in the initial sample and Fig. 8b shows the plate with no CFU just after two hours of the photooxidation.

### 3 Conclusions

We have developed a novel photocatalytic system where a highly energy-efficient UV-LED light source is used, thus significantly reducing the cost of operation compared to other technologies. We are also employing a nanoporous TiO<sub>2</sub> structure in our system which enhances the surface area of the photocatalyst tremendously, resulting in further performance improvement of the device. These nanomaterials are part of the substrate thus providing them enhanced durability as compared to powdered photocatalysts which are adhered to the substrate by various methods and are prone to break loose and causing secondary pollution.

Another innovative idea in our approach is the synergistic use of photocatalysis and wet scrubbing. The oxygen concentration plays a very significant role in photocatalysis. The thin water film design coupled with the wet scrubbing to keep the system well-oxygenated results in a low electron-hole recombination rate and high photocatalytic performance.

Employment of 365 nm UVA-LED also helps in decreasing the energy cost and significantly increasing the photocatalytic activity of the system. This LED-based technology also helps in reducing the dependence on mercury-based UV lamps thus decreasing the environmental pollution. The experimental results obtained through the photocatalytic oxidation of organic and biological pollutants in our study indicate that a highly efficient system is manufactured which can be

employed in various green environmental applications such as water, wastewater, and air purification technologies.

## 4 Experimental

### 4.1 Materials and chemicals

Titanium metal tubes with different diameters were purchased from Ticon Industries (Leander, Texas, USA). Hydrochloric acid (38%), ethylene glycol, methylene blue, acetone, and ammonium fluoride were purchased from Sigma Aldrich and used as is.

### 4.2 Fabrication of nanoporous TiO<sub>2</sub>

The highly ordered nanoporous TiO<sub>2</sub> was initially grown using an anodization process in a one-compartment two-electrode cell that contained ethylene glycol + 0.3 wt% NH<sub>4</sub>F + 2 wt% H<sub>2</sub>O, with a Ti tube as the anode, and a titanium mesh coil as the cathode, respectively. Briefly, the Ti tube was initially sonicated in acetone for 15 min, after which it was etched in 18% HCl at 85 °C for 10 min. Subsequently, the etched Ti tube was anodized at 50 V over 5 h, after which the rough as-grown nanoporous TiO<sub>2</sub> layer was removed by applying masking tape. Second anodization was performed where 50 V was applied for 15 minutes resulting in the formation of uniform nanoporous TiO<sub>2</sub>. Finally, to achieve the anatase phase of the material, the anodized Ti was annealed in an oven at 450 °C for 3 h.

### 4.3 Characterization of the synthesized Nanoporous TiO<sub>2</sub>

The synthesized nanoporous TiO<sub>2</sub> was characterized by energy-dispersive X-ray spectroscopy (EDX), and scanning electron microscopy (SEM, Hitachi-S400). X-ray diffraction (XRD) measurements were done on a PANalytical Empyrean system using a Cu (K $\alpha$ , 1.5406 Å). An LED assembly containing 365 nm UVA LEDs was employed for the irradiation of the nanoporous TiO<sub>2</sub>. The UV light, with an intensity of 500 mW cm<sup>-2</sup>, directly irradiated the surface of the wet photocatalyst.

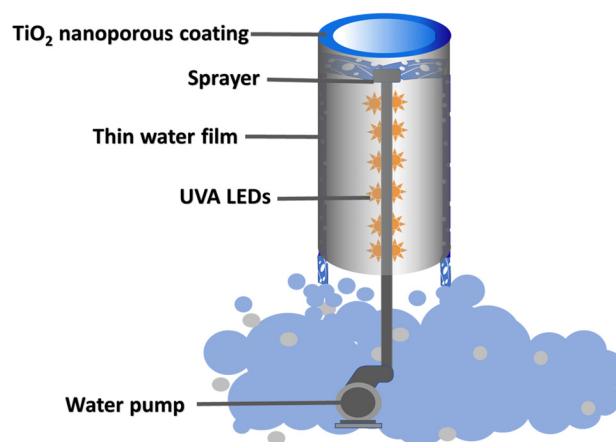


**Fig. 9** Design of the photoreactor.





#### 4.4 Photocatalytic reactor

The diagram of the photoreactor is shown in Fig. 9. In a typical setup, the photocatalytic reactor was made up of a titanium tube with the as-grown TiO<sub>2</sub> nanoporous material on the inner surface. This tube is held in place with the help of an assembly which has a pump attached to it at the bottom. A stainless-steel pipe runs through the middle of the titanium tube and connects the pump at the bottom to the sprayer at the top. When running, the sprayer pushes the water violently initiating water scrubbing of the air and this water then runs down as a thin film on the TiO<sub>2</sub> nanoporous material inside the titanium tube. The UVA-LED assembly is secured in a glass tube wrapped around the stainless-steel pipe and irradiates the whole inner surface of the titanium tube. The LED assembly is centrally located and thus provides an ideal irradiation to the surrounding nanoporous photocatalyst. The treated water after the photo-oxidation process falls back into the reservoir.

#### 4.5 Photocatalytic activity measurements

The photocatalytic activity of synthesized nanoporous TiO<sub>2</sub> was evaluated by measuring the photocatalytic degradation of methylene blue MB (representing an organic dye pollutant) under irradiation. The reactor is a cylindrical titanium tube with an inner surface coated with TiO<sub>2</sub> nanoporous material. The MB solution was prepared by dissolving 20 mg of MB in 6 L of tap water. The reaction mixture was stirred for 30 min in the absence of light in order to obtain a homogeneous dissolution of dye in the water and to achieve an adsorption-desorption equilibrium. The light source was a 365 nm LED strip 3 cm away from the TiO<sub>2</sub> surface. The UV intensity on the TiO<sub>2</sub> surface was measured to be 500 mW cm<sup>-2</sup>. Samples were collected from the reaction mixture at regular intervals. The samples were used to measure the degradation of MB using a UV-vis spectrometer (Analytik Jena Spekol 1500). After taking the reading the solution was added back to the reactor.

### Conflicts of interest

The prototypes were built based on the IP provided by John B. Hayden (WaterDrape LLC) through his patents (US 10329180B2 and European Patent No. 3395450). Dr. Sapanbir S. Thind is a consultant of WaterDrape LLC.

### Acknowledgements

We acknowledge 1219441BC Ltd and NRC IRAP for providing funding to test this technology. JSM thanks Mitacs Canada for Accelerate Fellowship funding for Dr. Mathias Paul. We also thank the Centre for Advanced Materials and Related Technology (CAMTEC) at The University of Victoria for the SEM, EDX, and XRD analysis.

### References

- 1 S. Senthilkumar, C. A. Basha, M. Perumalsamy and H. J. Prabhu, Electrochemical oxidation and aerobic biodegradation with isolated bacterial strains for dye wastewater: Combined and integrated approach, *Electrochim. Acta*, 2012, **77**, 171–178.
- 2 K. Abuhasel, M. Kchaou, M. Alquraish, Y. Munusamy and Y. T. Jeng, Oily wastewater treatment: Overview of conventional and modern methods, challenges, and future opportunities, *Water*, 2021, **13**, 980.
- 3 S. Hakak, W. Z. Khan, G. A. Gilkar, N. Haider, M. Imran and M. S. Alkathiri, Industrial wastewater management using blockchain technology: Architecture, requirements, and future directions, *IEEE Internet Things Mag.*, 2020, **3**, 38–43.
- 4 *The United Nations World Water Development Report 2017: Wastewater the Untapped Resource*, UNESCO, Paris France, 2017.
- 5 S. Singh, R. Sharma and M. Khanuja, A review and recent developments on strategies to improve the photocatalytic elimination of organic dye pollutants by BiOX (X=Cl, Br, I, F) nanostructures, *Korean J. Chem. Eng.*, 2018, **35**, 1955–1968.
- 6 T. Robinson, G. McMullan, R. Marchant and P. Nigam, Remediation of dyes in textile effluent: A critical review on current treatment technologies with a proposed alternative, *Bioresour. Technol.*, 2001, **77**, 247–255.
- 7 G. Ren, H. Han, Y. Wang, S. Liu, J. Zhao, X. Mengand and Z. Li, Recent advances of photocatalytic application in water treatment: A review, *Nanomaterials*, 2021, **11**, 1804.
- 8 H. Zhao, H. Li, H. Yu, H. Chang, X. Quan and S. Chen, CNTs-TiO<sub>2</sub>/Al<sub>2</sub>O<sub>3</sub> composite membrane with a photocatalytic function: Fabrication and energetic performance in water treatment, *Sep. Purif. Technol.*, 2013, **116**, 360–365.
- 9 S. Pandey, K. K. Mandari, J. Kim, M. Kang and E. Fosso-Kankeu, Recent advancement in visible-light-responsive photocatalysts in heterogeneous photocatalytic water treatment technology, in *Photocatalysts in Advanced Oxidation Processes for Wastewater Treatment*, Scrivener Publishing, Massachusetts, 2020.
- 10 S. N. Ahmed and W. Haider, Heterogeneous photocatalysis and its potential applications in water and wastewater treatment: A review, *Nanotechnology*, 2018, **29**, 342001.
- 11 F. Biancullo, N. F. F. Moreira, A. R. Ribeiro, C. M. Manaia, J. L. Faria, O. C. Nunes, S. M. Castro-Silva and A. M. T. Silva, Heterogeneous photocatalysis using UVA-LEDs for the removal of antibiotics and antibiotic-resistant bacteria from urban wastewater treatment plant effluents, *Chem. Eng. J.*, 2019, **367**, 304–313.
- 12 K. Wetchakun, N. Wetchakun and S. Sakulsermsuk, An overview of solar/visible light-driven heterogeneous photocatalysis for water purification: TiO<sub>2</sub>- and ZnO-based photocatalysts used in suspension photoreactors, *J. Ind. Eng. Chem.*, 2019, **71**, 19–49.
- 13 M. Mokhtarifar, D. T. Nguyen, M. V. Dimanti, R. Kaveh, M. Asa, M. Sakar, M. P. Pedferri and T. O. Do, Fabrication of



- dual-phase  $\text{TiO}_2/\text{WO}_3$  with post-illumination photocatalytic memory, *New J. Chem.*, 2020, **44**, 20375–20386.
- 14 M. Sakar, R. M. Prakash and T. O. Do, Insights into the  $\text{TiO}_2$ -based photocatalytic systems and their mechanisms, *Catalysis*, 2019, **9**, 680.
  - 15 S. K. Loeb, P. J. J. Alvarez, J. A. Brame, E. L. Cates, W. Choi, J. Crittenden, D. D. Dionysiou, Q. Li, G. Li-Puma, X. Quan, D. L. Sedlak, T. David Waite, P. Westerhoff and J.-H. Kim, The technology horizon for photocatalytic water treatment: Sunrise or sunset?, *Environ. Sci. Technol.*, 2019, **53**, 2937–2947.
  - 16 X. Chen and S. S. Mao, Titanium dioxide nanomaterials: Synthesis, properties, modifications, and applications, *Chem. Rev.*, 2007, **107**, 2891–2959.
  - 17 S. Dong, J. Feng, M. Fan, Y. Pi, L. Hu, X. Han, M. Liu, J. Sun and J. Sun, Recent developments in heterogeneous photocatalytic water treatment using visible light-responsive photocatalysts: A review, *RSC Adv.*, 2015, **5**, 14610–14630.
  - 18 Y. Qu and X. Duan, Progress, challenge and perspective of heterogeneous photocatalysts, *Chem. Soc. Rev.*, 2013, **42**, 2568–2580.
  - 19 D. Hong, A. Sharma, D. Jiang, E. Stellino, T. Ishiyama, P. Postorino, E. Placidi, Y. Kon and K. Koga, Laser ablation nanoarchitectonics of Au–Cu alloys deposited on  $\text{TiO}_2$  photocatalyst films for switchable hydrogen evolution from formic acid dehydrogenation, *ACS Omega*, 2022, **7**, 31260–31270.
  - 20 N. S. Ibrahim, W. L. Leaw, D. Mohamad, S. H. Alias and H. Nur, A critical review of metal-doped  $\text{TiO}_2$  and its structure–physical properties–photocatalytic activity relationship in hydrogen production, *Int. J. Hydrogen Energy*, 2020, **45**, 28553–28565.
  - 21 Y. Cherif, H. Azzi, K. Sridharan, S. Ji, H. Choi, M. G. Allan, S. Benaissa, K. Saidi-Bendahou, L. Dampsey, C. S. Ribeiro, S. Krishnamurthy, S. Nagarajan, M. M. Maroto-Valer, M. F. Kuehnelt and S. Pitchaimuthu, Facile synthesis of gram-scale mesoporous  $\text{Ag}/\text{TiO}_2$  photocatalysts for pharmaceutical water pollutant removal and green hydrogen generation, *ACS Omega*, 2023, **8**, 1249–1261.
  - 22 Y. Dong, X. Ji, A. Laaksonen, X. Lu and S. Zhang, Excellent trace detection of proteins on  $\text{TiO}_2$  nanotube substrates through novel topography optimization, *J. Phys. Chem. C*, 2020, **124**, 27790–27800.
  - 23 J. Zhang, L. Li, Z. Xiao, D. Liu, S. Wang, J. Zhang, Y. Hao and W. Zhang, Hollow sphere  $\text{TiO}_2\text{--ZrO}_2$  prepared by self-assembly with polystyrene colloidal template for both photocatalytic degradation and  $\text{H}_2$  evolution from water splitting, *ACS Sustainable Chem. Eng.*, 2016, **4**, 2037–2046.
  - 24 S. S. Thind, G. Wu and A. Chen, Synthesis of mesoporous nitrogen–tungsten co-doped  $\text{TiO}_2$  photocatalysts with high visible light activity, *Appl. Catal., B*, 2012, **111–112**, 38–45.
  - 25 A. B. Holmes, D. Khan, D. O. Livera and F. Gu, Enhanced photocatalytic selectivity of noble metallized  $\text{TiO}_2$  nanoparticles for the reduction of selenate in water: Tunable Se reduction product  $\text{H}_2\text{Se(g)}$  vs.  $\text{Se(s)}^\pm$ , *Environ. Sci.: Nano*, 2020, **7**, 1841–1852.
  - 26 A. Crake, K. C. Christoforidis, R. Godin, B. Moss, A. Kafizas, S. Zafeiratos, J. R. Durrant and C. Petit, Titanium dioxide/carbon nitride nanosheet nanocomposites for gas phase  $\text{CO}_2$  photoreduction under UV-visible irradiation, *Appl. Catal., B*, 2019, **242**, 369–378.
  - 27 A. B. Holmes, A. Ngan, J. Ye and F. Gu, Selective photocatalytic reduction of selenate over  $\text{TiO}_2$  in the presence of nitrate and sulfate in mine-impacted water, *Chemosphere*, 2022, **287**, 131951.
  - 28 J. Huang, H. Ren, X. Liu, X. Li and J.-J. Shim, Facile synthesis of porous  $\text{TiO}_2$  nanospheres and their photocatalytic properties, *Superlattices Microstruct.*, 2015, **81**, 16–25.
  - 29 W. Zhang, Y. Xie, D. Xiong, X. Zeng, Z. Li, M. Wang, Y.-B. Cheng, W. Chen, K. Yan and S. Yang,  $\text{TiO}_2$  Nanorods: A facile size- and shape-tunable synthesis and effective improvement of charge collection kinetics for dye-sensitized solar cells, *ACS Appl. Mater. Interfaces*, 2014, **6**, 9698–9704.
  - 30 J. Song, R. Guan, M. Xie, P. Dong, X. Yang and J. Zhang, Advances in electrospun  $\text{TiO}_2$  nanofibers: Design, construction, and applications, *Chem. Eng. J.*, 2022, **431**, 134343.
  - 31 J. Jitputti, Y. Suzuki and S. Yoshikawa, Synthesis of  $\text{TiO}_2$  nanowires and their photocatalytic activity for hydrogen evolution, *Catal. Commun.*, 2008, **9**, 1265–1271.
  - 32 N. Suriyachai, S. Chuangchote, N. Laosiripojana, V. Champreda and T. Sagawa, Synergistic effects of Co-doping on photocatalytic activity of titanium dioxide on glucose conversion to value-Added chemicals, *ACS Omega*, 2020, **5**, 20373–20381.
  - 33 A. T. Kuvarega, R. W. M. Krause and B. B. Mamba, Nitrogen/palladium-codoped  $\text{TiO}_2$  for efficient visible light photocatalytic dye degradation, *J. Phys. Chem. C*, 2011, **115**, 22110–22120.
  - 34 S. S. Thind, G. Wu, M. Tian and A. Chen, Significant enhancement in the photocatalytic activity of N, W co-doped  $\text{TiO}_2$  nanomaterials for promising environmental applications, *Nanotechnology*, 2012, **23**, 475706.
  - 35 H. Liu, S. S. Thind, G. Wu, J. Wen and A. Chen, Synthesis and photoelectrochemical studies of N, Zr co-doped mesoporous titanium dioxide, *J. Electroanal. Chem.*, 2015, **736**, 93–100.
  - 36 N. P. Chadwick, A. Kafizas, R. Quesada-Cabrera, C. Sotelo-Vazquez, S. M. Bawaked, M. Mokhtar, S. A. Al Thabaiti, A. Y. Obaid, S. N. Basahel, J. R. Durrant, C. J. Carmalt and I. P. Parkin, Ultraviolet radiation induced dopant loss in a  $\text{TiO}_2$  photocatalyst, *ACS Catal.*, 2017, **7**, 1485–1490.
  - 37 P. S. Mukherjee and A. K. Ray, Major challenges in the design of a large-scale photocatalytic reactor for water treatment, *Chem. Eng. Technol.*, 1999, **22**, 253–260.
  - 38 T. S. Natarajan, K. Natarajan, H. C. Bajaj and R. J. Tayade, Energy efficient UV-LED source and  $\text{TiO}_2$  nanotube array-based reactor for photocatalytic application, *Ind. Eng. Chem. Res.*, 2011, **50**, 7753–7762.
  - 39 P. K. Surolia, M. A. Lazar, R. J. Tayade and R. V. Jasra, Photocatalytic degradation of 3,3'-dimethylbiphenyl-4,4'-



- diamine (o-Tolidine) over nanocrystalline TiO<sub>2</sub> synthesized by sol-gel, solution combustion, and hydrothermal methods, *Ind. Eng. Chem. Res.*, 2008, **47**, 5847–5855.
- 40 J. Long, Mercury poisoning fatal to chemist, *Chem. Eng. News*, 1997, **75**, 11–12.
  - 41 M. Nabi, J. Wang, M. Meyer, M.-N. Croteau, N. Ismail and M. Baalousha, Concentrations and size distribution of TiO<sub>2</sub> and Ag engineered particles in five wastewater treatment plants in the United States, *Sci. Total Environ.*, 2021, **753**, 142017.
  - 42 D. Wang and L. Liu, Continuous fabrication of free-standing TiO<sub>2</sub> nanotube array membranes with controllable morphology for depositing interdigitated heterojunctions, *Chem. Mater.*, 2010, **22**, 6656–6664.
  - 43 G. K. Mor, K. Shankar, M. Paulose, O. K. Varghese and C. A. Grimes, Use of highly-ordered TiO<sub>2</sub> nanotube arrays in dye-sensitized solar cells, *Nano Lett.*, 2006, **6**, 215–218.
  - 44 Y. Zhao, H. Zhang, A. Liu, Y. Jiao, J.-J. Shim and S. Zhang, Fabrication of nanoarchitected TiO<sub>2</sub>(B)/C/rGO electrode for 4 V quasi-solid-state nanohybrid supercapacitors, *Electrochim. Acta*, 2017, **258**, 343–352.
  - 45 P. Roy, S. Berger and P. Schmuki, TiO<sub>2</sub> nanotubes: Synthesis and applications, *Angew. Chem., Int. Ed.*, 2011, **50**, 2904–2939.
  - 46 N. K. Allam and C. A. Grimes, Effect of rapid infrared annealing on the photoelectrochemical properties of anodically fabricated TiO<sub>2</sub> nanotube arrays, *J. Phys. Chem. C*, 2009, **113**, 7996–7999.
  - 47 X. Zeng, Y. X. Gan, E. Clark and L. Su, Amphiphilic and photocatalytic behaviors of TiO<sub>2</sub> nanotube arrays on Ti prepared via electrochemical oxidation, *J. Alloys Compd.*, 2011, **509**, L221–L227.
  - 48 Y. Chen, Y. Tang, S. Luo, C. Liu and Y. Li, TiO<sub>2</sub> nanotube arrays co-loaded with Au nanoparticles and reduced graphene oxide: Facile synthesis and promising photocatalytic application, *J. Alloys Compd.*, 2013, **578**, 242–248.
  - 49 P. Eskandari, M. Farhadian, A. R. S. Narar and B.-H. Jeon, Adsorption and photodegradation efficiency of TiO<sub>2</sub>/Fe<sub>2</sub>O<sub>3</sub>/PAC and TiO<sub>2</sub>/Fe<sub>2</sub>O<sub>3</sub>/zeolite nanophotocatalysts for the removal of cyanide, *Ind. Eng. Chem. Res.*, 2019, **58**, 2099–2112.
  - 50 P. S. Basavarajappa, S. B. Patil, N. Ganganagappa, K. R. Reddy, A. V. Raghu and C. V. Reddy, Recent progress in metal-doped TiO<sub>2</sub>, non-metal doped/codoped TiO<sub>2</sub> and TiO<sub>2</sub> nanostructured hybrids for enhanced photocatalysis, *Int. J. Hydrogen Energy*, 2020, **45**, 7764–7778.
  - 51 M. H. Suhag, I. Tateishi, M. Furukawa, H. Katsumata, A. Khatun and S. Kaneco, Application of Rh/TiO<sub>2</sub> nanotube array in photocatalytic hydrogen production from formic acid solution, *J. Compos. Sci.*, 2022, **6**, 327.
  - 52 S. Ozkan, N. T. Nguyen, A. Mazare and P. Schmuki, Optimized spacing between TiO<sub>2</sub> nanotubes for enhanced light harvesting and charge transfer, *ChemElectroChem*, 2018, **5**, 3183–3190.
  - 53 Q. Huang, T. Gao, F. Niu, D. Chen, Z. Chen, L. Qin, X. Sun, Y. Huang and K. Shu, Preparation and enhanced visible-light driven photocatalytic properties of Au-loaded TiO<sub>2</sub> nanotube arrays, *Superlattices Microstruct.*, 2014, **75**, 890–900.
  - 54 S. Zhang, H. Wang, M. Yeung, Y. Fang, H. Yu and F. Peng, Cu(OH)<sub>2</sub>-modified TiO<sub>2</sub> nanotube arrays for efficient photocatalytic hydrogen production, *Int. J. Hydrogen Energy*, 2013, **38**, 7241–7245.
  - 55 S. Kumar, T. Vats, S. N. Sharma and J. Kumar, Investigation of annealing effects on TiO<sub>2</sub> nanotubes synthesized by a hydrothermal method for hybrid solar cells, *Optik*, 2018, **171**, 492–500.
  - 56 T.-S. Kang, A. P. Smith, B. E. Taylor and M. F. Durstock, Fabrication of highly-ordered TiO<sub>2</sub> nanotube arrays and their use in dye-sensitized solar cells, *Nano Lett.*, 2009, **9**, 601–606.
  - 57 Y. Lin, Q. Qian, Z. Chen, D. Feng, P. D. Tuan and F. Yin, Surface modification of TiO<sub>2</sub> nanotubes prepared by porous titanium anodization via hydrothermal reaction: A method for synthesis high-efficiency adsorbents of recovering Sr ions, *Langmuir*, 2022, **38**, 11354–11361.
  - 58 M. Chu, Y. Tang, N. Rong, X. Cui, F. Liu, Y. Li, C. Zhang, P. Xiao and Y. Zhang, Hydrothermal synthesis, and tailoring the growth of Ti-supported TiO<sub>2</sub> nanotubes with thick tube walls, *Mater. Des.*, 2016, **97**, 257–267.
  - 59 F. Wei, Z. Chen, Y. Lin, Q. Qian, H. Jiang, P. Su, D. Liao and D. Feng, Characteristics of TiO<sub>2</sub> nanotubes fabricated by high-frequency cyclic anodization, *J. Electrochem. Soc.*, 2021, **168**, 036504.
  - 60 A. Shoja, A. Nourmohammadi and M. H. Feiz, Growth of TiO<sub>2</sub> nanotube arrays in semiconductor porous anodic alumina templates, *J. Mater. Res.*, 2014, **29**, 2432–2440.
  - 61 S. Minagar, C. C. Berndt, J. Wang, E. Ivanova and C. Wen, Review of the application of anodization for the fabrication of nanotubes on metal implant surfaces, *Acta Biomater.*, 2012, **8**, 2875–2888.
  - 62 Y. Yang, Y. Li and M. Pritzker, Morphological evolution of anodic TiO<sub>2</sub> nanotubes, *RSC Adv.*, 2014, **4**, 35833–35843.
  - 63 H. Cheng, J. Wang, Y. Zhao and X. Han, Effect of phase composition, morphology, and specific surface area on the photocatalytic activity of TiO<sub>2</sub> nanomaterials, *RSC Adv.*, 2014, **4**, 47031–47038.
  - 64 R. M. S. Sendão, J. C. G. Esteves da Silva and L. Pinto da Silva, Photocatalytic removal of pharmaceutical water pollutants by TiO<sub>2</sub> – carbon dots nanocomposites: A review, *Chemosphere*, 2022, **301**, 134731.
  - 65 M. Carballa, F. Omil, J. M. Lema, M. A. Llompart, C. García-Jares, I. Rodríguez, M. Gómez and T. Ternes, Behavior of pharmaceuticals, cosmetics and hormones in a sewage treatment plant, *Water Res.*, 2004, **38**, 2918–2926.
  - 66 P. R. Ginimuge and S. D. Jyothi, Methylene blue: Revisited, *J. Anaesthesiol., Clin. Pharmacol.*, 2010, **26**, 517–520.
  - 67 D. Chang, L. Sharma, C. S. Dela Cruz and D. Zhang, Clinical epidemiology, risk factors, and control strategies of Klebsiella pneumoniae infection, *Front. Microbiol.*, 2021, **12**, 750662.
  - 68 R. Duan, J. Liang, G. Shi, Z. Cui, R. Hai, P. Wang, Y. Xiao, K. Li, H. Qiu, W. Gu, X. Du, H. Jing and X. Wang, Homology



- analysis of pathogenic *Yersinia* species *Yersinia enterocolitica*, *Yersinia pseudotuberculosis*, and *Yersinia pestis* based on multilocus sequence typing, *J. Clin. Microbiol.*, 2014, **52**, 20–29.
- 69 W. A. Mitch, A. C. Gerecke and D. L. Sedlak, A N-nitrosodimethylamine (NDMA) precursor analysis for chlorination of water and wastewater, *Water Res.*, 2003, **37**, 3733–3741.
- 70 P. Westerhoff, Y. Yoon, S. Snyder and E. Wert, Fate of endocrine-disruptor, pharmaceutical, and personal care product chemicals during simulated drinking water treatment processes, *Environ. Sci. Technol.*, 2005, **39**, 6649–6663.
- 71 W. Lee, P. Westerhoff and J.-P. Croué, Dissolved organic nitrogen as a precursor for chloroform, dichloroacetonitrile, N-nitrosodimethylamine, and trichloronitromethane, *Environ. Sci. Technol.*, 2007, **41**, 5485–5490.

